Journal of Non-Crystalline Solids 407 (2015) 184–189

Contents lists available at ScienceDirect

Journal of Non-Crystalline Solids

journal homepage: www.elsevier.com/ locate/ jnoncrysol

Dynamics of poly(propyl methacrylate) as a function of temperature and pressure

Panagiotis Panagos, George Floudas *

University of Ioannina, Department of Physics, 451 10 Ioannina, Greece

ARTICLE INFO

Article history:
Received 1 July 2014
Received in revised form 30 July 2014
Available online 11 September 2014

Keywords:
Segmental dynamics;
Pressure dependence;
Poly(propyl methacrylate)

ABSTRACT

The local segregation and dynamics of poly(propyl methacrylate) (PPMA) are studied as a function of temperature by X-rays and by dielectric spectroscopy and rheology, respectively. Pressure is employed in dielectric spectroscopy for investigating the origin of segmental dynamics and for separating the segmental from the faster β-process. The segmental dynamics of PPMA is controlled mainly by temperature via the intramolecular barriers. The pressure coefficient of the glass temperature is one of the lowest ever reported ($dT_g/dP = 150$ K/GPa). Based on this finding we examined a possible correlation between the values of the ratio of the apparent activation energy.

1. Introduction

Poly(*n*-alkyl methacrylates) are composed from a PMMA-like backbone and a PE-like side group and as a consequence display interesting structural and dynamic properties [1–12]. Structurally the side groups are segregated from the backbones forming their own "domains". In this respect, they can be considered as composite "materials" at the nano-scale. This tendency for nano-phase segragation is more evident in the higher alkyl methacrylates, such as poly(octadecyl methacrylate) (PODMA), with the crystallization of the side groups at atmospheric pressure [13] and at elevated pressures [14].

Apart from these unique structural features, poly(*n*-alkyl methacrylates) can be considered as model systems in studying the origin of the segmental dynamics and the respective freezing of the dynamics at the liquid-to-glass temperature, T_g, by systematically varying the length of the side group. Herein we investigate, respectively, the structure and dynamics of poly(propyl methacrylate) (PPMA) as a function of temperature and pressure by X-rays and by dielectric spectroscopy and rheology. With these tools we explore the influence of local segregation on the dynamic properties of PPMA. More specifically, we are studying the origin of the segmental dynamics by exploring the contribution from thermally activated processes (by crossing the intra-molecular barriers) and of free-volume (inter-molecular correlations). We find that despite the local phase segregation between side groups and backbones the segmental dynamics are mainly of intramolecular origin. The information on the relative contribution of volume (density) and thermal energy to the segmental dynamics near T_g is then assumed to be reflected also in the pressure sensitivity of T_g. By examining values from all available polymers a broad correlation between the two quantities is shown.

2. Experimental part

2.1. Sample

The PPMA sample employed in the present study was purchased from Polymer Source Inc. It was prepared by radical polymerization and had a weight-averaged degree of polymerization of $M_w = 48 \times 10^3$ g/mol ($M_w/M_n \sim 1.2$).

2.2. Rheology

A TA Instruments rheometer (model AR-G2) with a magnetic bearing that allows for low nano-torque control was used for recording the viscoelastic properties of PPMA. Measurements were made with the environmental test chamber as a function of temperature. The sample was prepared on the bottom plate of a 25 mm diameter parallel plate geometry and heated under nitrogen atmosphere until it could flow. Subsequently, the upper plate was brought into contact, the gap thickness was adjusted and the sample was slowly cooled to the desired starting temperature. The storage (G′) and loss (G′′) shear moduli were monitored in isothermal frequency scans for temperatures in the range of 328–433 K and for frequencies in the range of $10^{-1} < \omega < 10^2$ rad s^{-1}.

2.3. X-ray scattering

Wide-angle X-ray scattering (WAXS) measurements were made at ambient temperature using Cu Kα radiation from a Rigaku MicroMax 007 X-ray generator ($\lambda = 1.54184$ nm), using Osmic Confocal Max-Flux

* Corresponding author.
E-mail address: gfloudas@uoi.gr (G. Floudas).

http://dx.doi.org/10.1016/j.jnoncrysol.2014.08.038
0022-3093/

curved multilayer optics. Diffraction patterns were obtained by radial averaging of the data recorded by a 2D-detector (Mar345 Image Plate).

2.4. Dielectric spectroscopy

The sample cell consisted of two electrodes, 20 mm in diameter and a thickness of 50 μm. Dielectric measurements were made at different temperatures in the range from 248.15 to 428.15 K, at atmospheric pressure, and for frequencies in the range from 1×10^{-2} to 1×10^{6} Hz using a Novocontrol Alpha system comprising a frequency response analyzer (Solartron Schlumberger FEA 1260) and a broadband dielectric converter with an active sample head. In addition, pressure-dependent measurements were made under "isothermal" conditions (the following temperatures were used: 303, 333, 338, 343, 353, 363, 373, 383, 393 K) and for pressures in the range from 0.1 to 300 MPa. The complex dielectric permittivity $\varepsilon^* = \varepsilon' - i\varepsilon''$, where ε' is the real and ε'' is the imaginary part, is a function of frequency ω, temperature T, and pressure P, $\varepsilon^* = \varepsilon^*(\omega, T, P)$ [15–17]. In the analysis of the DS spectra we have used the empirical equation of Havriliak and Negami (HN) [18]

$$\varepsilon^*_{HN}(\omega, T) = \varepsilon_\infty(T) + \frac{\Delta\varepsilon(T)}{[1 + (i\omega \cdot \tau_{HN}(T))^m]^n} + \frac{\sigma_0(T)}{i\varepsilon_f\omega} \quad (1)$$

where $\tau_{HN}(T,P)$ is the characteristic relaxation time, $\Delta\varepsilon(T,P) = \varepsilon_0(T,P) - \varepsilon_\infty(T,P)$ is the relaxation strength of the process under investigation, m, n (with limits $0 < m$, $mn \leq 1$) describe, respectively, the symmetrical and unsymmetrical broadening of the distribution of relaxation times, σ_0 is the dc-conductivity and ε_f is the permittivity of the free space. In the fitting procedure, we have used the ε'' values at every temperature and pressure and in some cases the ε' data were also used as a consistency check. From, τ_{HN} the relaxation time at maximum loss, τ_{max}, is obtained analytically following:

$$\tau_{max} = \tau_{HN} \cdot \sin^{-1/m}\left(\frac{\pi m}{2(1+n)}\right) \cdot \sin^{1/m}\left(\frac{\pi mn}{2(1+n)}\right) \quad (2)$$

In the temperature range where two relaxation processes (α and β) contribute to ε^* there are two ways of representing the data. The first one, followed here, is based in a summation of two HN functions and assumes statistical independence in the frequency domain. The second one, proposed by Williams and Watts is a molecular theory for the dipole moment time–correlation function $C_\mu(t)$ (also known as "Williams ansatz" [19]). An alternative representation of the dielectric data is through the inverse of the dielectric permittivity $\varepsilon^*(\omega)$ *i.e.*, the electric modulus, which is related to the dielectric permittivity through

$$M^*(\omega) = \frac{1}{\varepsilon^*(\omega)} = M' + iM'' \quad (3)$$

In Eq. (3), M' and M'' are the real and imaginary parts of the electric modulus, respectively. The electric modulus representation, $M^*(\omega)$, is an absolute necessity in cases where a comparison with rheology data is needed as in the present here. The relaxation times obtained from the electric modulus ($\tau_M{}^*$) and the complex permittivity ($\tau_\varepsilon{}^*$) representations scale as [17]

$$\tau_{M''} \sim \tau_{\varepsilon''}\left(1 + \frac{\Delta\varepsilon}{\varepsilon_\infty}\right)^{-1/\alpha} \quad (4)$$

and can differ substantially in systems with a high dielectric strengths.

2.5. Pressure–volume–temperature

Literature values were used for the *PVT* equation of state. The Tait equation of state was employed [20]

$$V(P,T) = V(0,T)\left\{1 - 0.0894 \ln\left[1 + \frac{P}{B(T)}\right]\right\} \quad (5)$$

where for $T > T_g$, the specific volume at atmospheric pressure is given by $V(0,T) = 0.908 + 6.7 \times 10^{-4} T - 5.4 \times 10^{-7} T^2$ (V in cm^3/g, T in °C) and $B(T) = (213.0\ \text{MPa}) \exp(-0.0043\ T)$ (T in °C).

3. Results

The results of the structural investigation (X-rays) are summarized in Fig. 1. The figure compiles WAXS curves from a series of poly(*n*-alkyl methacrylates) with increasing number of carbon atoms on the alkyl chain [7,21]. With the exception of PMMA, all poly(*n*-alkyl methacrylates) display three peaks. The first one is the usual van der Waals (VDW) peak due to contacts of atoms. The second, at lower wavevectors, is the low van der Waals (LVDW) peak reflecting interchain correlations. This feature is evident when plotting the

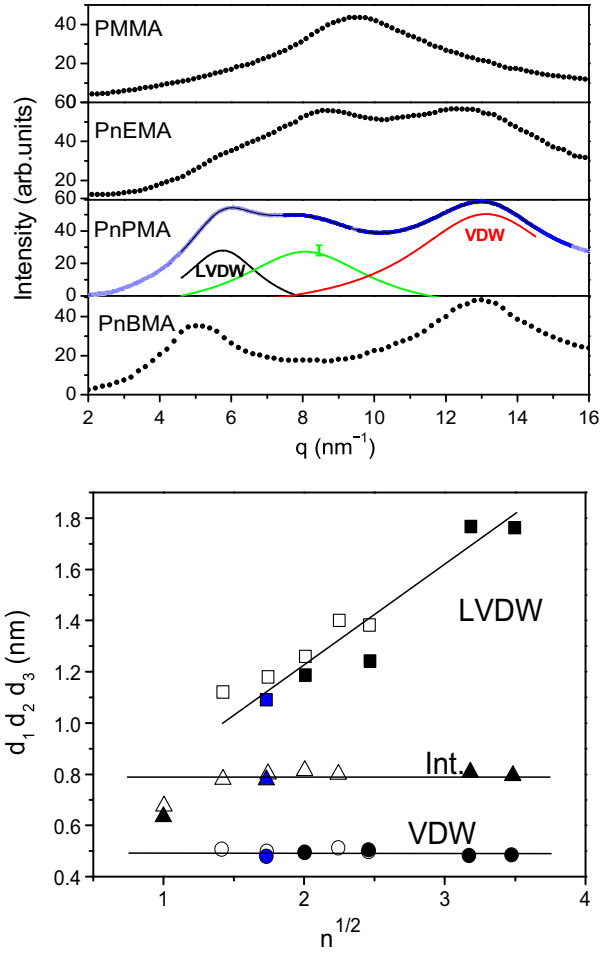

Fig. 1. (Top): WAXS patterns from a series of lower poly(*n*-alkyl methacrylates) with $n = 1$ (PMMA), $n = 2$ (PnEMA), $n = 3$ (PnPMA) and $n = 4$ (PnBMA) at 293 K. The procedure of curve de-convolution into three main components is shown for PnPMA (VDW: is the main van der Waals peak, LVDW: is the lower van der Waals peak and I: is the intermediate component. (Bottom): Dependence of the equivalent Bragg spacings on the square root of the number of alkyl side-group carbon atoms: VDW (spheres), LVDW (squares), Int. (triangles). Open symbols from ref. [21]. Filled symbols from ref. [7]. Blue symbols: current work.

corresponding equivalent Bragg distance (as $d = 2\pi/q^*$) as a function of $n^{1/2}$, where n is the number of carbon atoms on the alkyl chain. It can be parameterized as $d_1 = d_0 + sn^{1/2}$ with typical values of $d_0 \sim 0.7$ nm and $s \sim 0.385$ nm/CH_2 [7]. The third peak is an intermediate feature that is more close to the single peak in PMMA. This picture for PPMA confirms the tendency for local segregation as found in other poly(n-alkyl methacrylates). In Fig. 1, we include literature data for all known poly(n-alkly methacrylates) [7,21] including the PPMA studied herein.

Fig. 2 provides some dielectric loss curves of PPMA at 0.1 MPa at different temperatures as indicated. A representative fit to a summation of two HN functions and to the dc-conductivity is indicated at $T = 348$ K. The two processes reflect the faster β-process and the slower α-process. Their origin will be discussed subsequently in view of their temperature and pressure dependence.

Rheology was employed that provides both the segmental and longer chain dynamics (Fig. 3). The figure depicts storage and loss curves that are shifted first horizontally with appropriate shift factors (a_T)—whose T-dependence is plotted in the inset—and subsequently vertically (with shift factors b_T) in the usual master-curve construction corresponding to a reference temperature of 373 K. Time–temperature superposition (tTs) works except in the vicinity of the glass temperature. The shift factors can be described with the Williams–Landel–Ferry (WLF) equation as:

$$\log a_T = -\frac{c_1^r(T-T_r)}{c_2^r + T - T_r} \tag{6}$$

where T_r is the reference temperature and c_1^r and c_2^r are the WLF coefficients at this temperature. These parameters at T_g assume the following values: $c_1{}^g = 15.2$ and $c_2{}^g = 63.3$ K. The master curve shows a plateau which is consistent with the relatively high molecular weight of the sample. Moreover, this feature is followed by a broad process at higher frequencies in the vicinity of the liquid-to-glass temperature.

The relaxation times obtained from rheology and DS can be discussed in the usual Arrhenius representation of Fig. 4. The relaxation times in the figure are obtained from the modulus representation (according to Eq. (4)). Notice that the DS segmental relaxation times are faster than the ones obtained from rheology. Despite this all sets can be fitted by the Vogel–Fulcher–Tammann (VFT) equation with appropriate parameters as:

$$\tau_{max} = \tau_0 exp\left(\frac{D_T T_0}{T - T_0}\right) \tag{7}$$

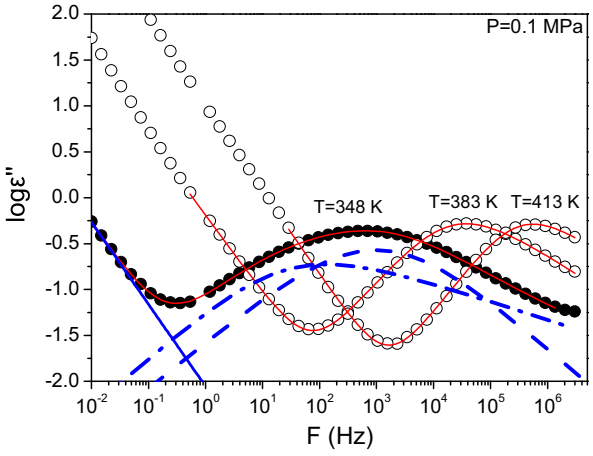

Fig. 2. Dielectric loss spectra of PPMA at 0.1 MPa for three representative temperatures. The deconvolution of the loss curve at 348 is shown with three contributions: the β-process (dashed line) at higher frequencies, the α-process at intermediate frequencies (dah-dotted line) and the conductivity contribution (dash-dotted line).

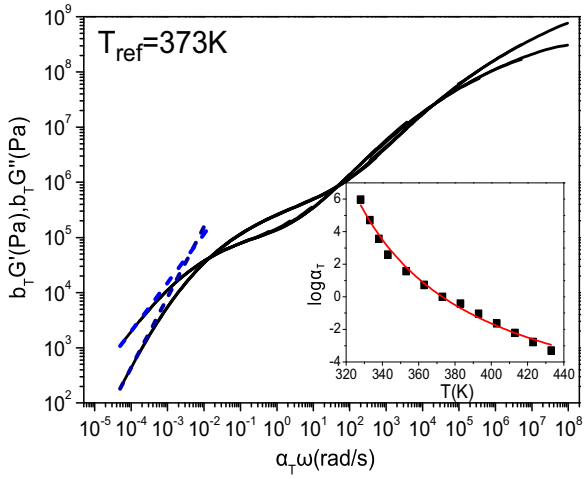

Fig. 3. Master curve for the storage and loss shear moduli of PPMA at a reference temperature of 373 K. The terminal relaxation times were obtained from the crossings of the lines with slopes 1 and 2 for the loss and storage moduli, respectively. In the inset the temperature dependence of the shift factors is shown together with the fit to the WLF equation.

where τ_0 is the relaxation time in the limit of very high temperature, D_T is a dimensionless parameter and T_0 is the "ideal" glass temperature. These parameters assume values of $\tau_0 = 2.1 \times 10^{-10}$ s, $D_T = 4.1 \pm 0.3$, and $T_0 = 279 \pm 2$ K for the DS segmental relaxation whereas $\tau_0 = 1.3 \times 10^{-11}$ s, $D_T = 7 \pm 2$, and $T_0 = 268 \pm 9$ K for the same relaxation in rheology.

The DS spectra are dominated by two "local" relaxation mechanisms. These can best be investigated under "isothermal" conditions with the application of pressure [3,8,22]. Pressure slows-down both modes but the effect is more pronounced for the segmental process as compared to the more local β-process. This is depicted in Fig. 5 where the segmental relaxation times are plotted as a function of pressure at four temperatures. In the same figure the β-process is also shown at several temperatures as indicated. The relaxation times corresponding to the α-process comply to the modified VFT equation [23] for pressure according to:

$$\tau_{max} = \tau_a exp\left(\frac{D_P P_0}{P_0 - P}\right) \tag{8}$$

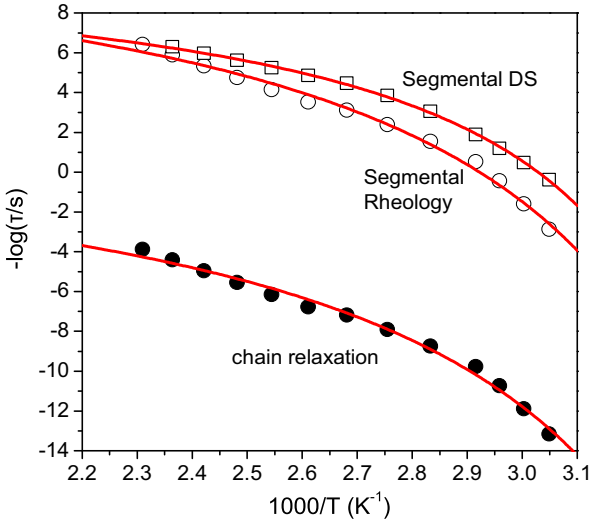

Fig. 4. Relaxation times corresponding to the dielectric segmental (α-) process (open squares) and to the segmental and terminal times (open and filled circles, respectively) obtained from rheology. All relaxation times are obtained from the modulus representation. Solid lines are fits to the VFT equation.

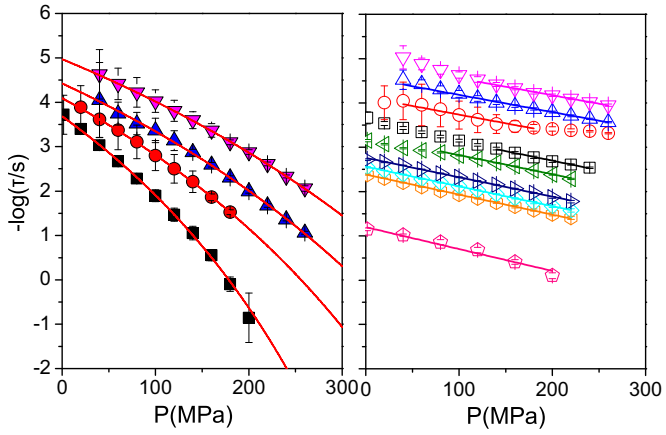

Fig. 5. Pressure dependence of the relaxation times at maximum loss for the segmental (α-) process (left) and the local β-process (right). The segmental times refer to (squares): 363 K, (circles): 373 K, (up triangles): 383 K and (down triangles): 393 K. The β-process times are at the following temperatures: (pentagons): 303 K, (hexagons): 333 K, (rhombi): 338 K, (right triangles); 343 K, (left triangles): 353 K, (squares): 363 K, (circles): 373 K, (up triangles): 383 K and (down triangles): 393 K. Lines are fits to the modified VFT equation for pressure (left) and to a linear pressure dependence (right).

where τ_α is the relaxation time at $P = 0.1$ MPa at a given temperature, D_P is a dimensionless parameter and P_0 is the pressure corresponding to the "ideal" glass temperature. P_0 assumes the following values for the different "isotherms" investigated: 670 ± 5 MPa; 890 ± 4 MPa, 1038 ± 7 MPa and 1162 ± 6 MPa at 363, 373, 383 and 393 K, respectively. The D_P value was held constant at 23.33 from a free fit to the 363 K data set. On the other hand, the β-process relaxation times display a much weaker pressure dependence that can be used to extract the apparent activation volume, $\Delta V^{\neq}$, [16] as:

$$\Delta V^{\neq}(T,P) = 2.303\,RT\left(\frac{\partial log\tau}{\partial P}\right)_T \tag{9}$$

This quantity is plotted in Fig. 6 for both processes as a function of temperature. For the β-process the single-valued slope at each temperature from Fig. 5 was used whereas for the α-process the initial slope (*i.e.*, the slope of $\tau(P)$ at $P \to 0$) was employed. Earlier studies from the Ioannina group identified [8,24–28] that $\Delta V^{\neq}$ has a strong T-dependence on approaching T_g whereas at $T >> T_g$ assumes values

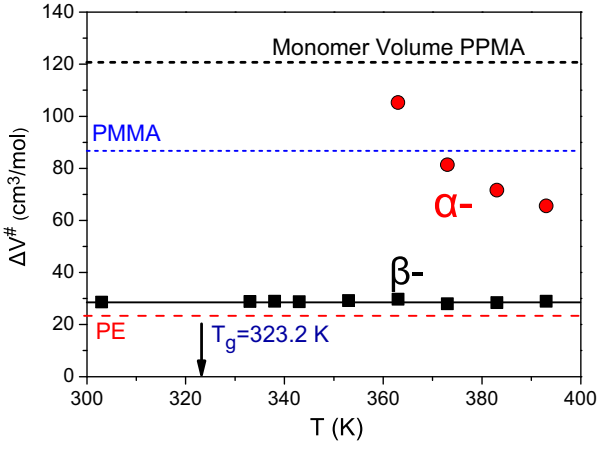

Fig. 6. Dependence of the apparent activation volume on temperature for the α-process (spheres) and β-process (squares) of PPMA. The dashed lines give the monomer volumes of PPMA (black), PMMA (blue) and PE (red), respectively.

comparable to the monomer volume (or better the repeat unit volume). This is also depicted in Fig. 6 for PPMA. The β-process shows a small and T-independent apparent activation volume with values comparable to the repeat unit volume of polyethylene. On the other hand, the α-process displays strong temperature dependence and approaches a value that is comparable to the repeat unit volume of PMMA. This in turn suggests that, dynamically speaking, PPMA can be considered as a composite material made of a PE-like side group and a PMMA-like backbone. The emerging dynamic picture is in agreement with the static picture (Fig. 1) as they both suggest local phase segregation between the side groups and the backbones [9].

4. Discussion

It has been discussed extensively in the literature that a critical test of the origin of the different processes associated with the liquid-to-glass dynamics and of the relative influence of volume (or density) and temperature is provided by the value of the ratio $\Re$ of the apparent activation energy at constant volume, $Q_V(T, V)$, to that at constant pressure, $Q_P(T, P)$ [3,8,24–31]

$$\Re = \left(\partial \ln\tau/\partial(1/T)_V\right)/\left(\partial \ln\tau/\partial(1/T)_P\right) = Q_V(T,V)/Q_P(T,P) \tag{10}$$

$\Re$ assumes values in the range $0 \le \Re < 1$ and provides a quantitative measure of the role of temperature and density on the dynamics. Values near unity suggest that the dynamics are governed mainly by the thermal energy (*i.e.*, by the intramolecular energy barriers pertinent to conformational changes) whereas values near zero suggest that free volume ideas prevail, since in that case, $Q_V = 0$. However, there exists not a single polymer or glass-forming liquid that has the extreme values of 0 or 1, suggesting that the picture is more complicated than the two extreme cases discussed above. The fact that all glass-forming systems show $Q_V \neq 0$ clearly shows that simple free-volume theories fail to describe the dynamics of glass-formers as a function of temperature and pressure.

Several different approaches have been suggested to obtain the ratio $\Re$ suggested by different groups and these are summarized in [8]. Subsequently, two ideas were explored that lead to a better understanding of the dynamics in the vicinity of the glass temperature. The first one was based on the feature of dynamics which is better known as the "thermodynamic scaling" [30–33]. The second approach emphasized the role of molecular volume and local packing on the glass "transition" dynamics [24]. With respect to the latter Floudas *et al.* [24] have shown that the repeat unit volume and local packing play a key role in controlling the value of this ratio at T_g, and thus the dynamics associated with the glass temperature. In particular, for *flexible* main-chain polymers, temperature, through the presence of energy barriers opposing molecular motions, is the main parameter affecting the dynamics whereas in polymers with *bulky side-groups* or in glass-forming liquids with large molar volumes, volume effects gain importance. A similar conclusion was reached by a recent theory of glass formation [34] whereas another method emphasized the importance of intermolecular cooperativity of motions (and fragility) [35].

For PPMA, we obtained $\Re$ through the density map shown in Fig. 7. The figure depicts all segmental relaxation times of PnPMA obtained both from the "isotherms" and the "isobars" as a function of density. Then the ratio $\Re$ can be obtained from the intersects of the "isotherms" and "isobars" as [8,29]

$$\frac{Q_V}{Q_P} \approx \frac{\Delta E^{\neq}}{\Delta H^{\neq}} = 1 - \left(\frac{\partial P}{\partial T}\right)_V \left(\frac{\partial T}{\partial P}\right)_\tau \tag{11}$$

where $(\partial P/\partial T)_V$ can be obtained from the equation of state and $(\partial T/\partial P)_\tau$ is the pressure coefficient of T_g. The latter can be obtained from Fig. 8 where the pressure dependence of the glass temperature of different poly(n-alkyl methacrylates) is given. In Fig. 8, all data are obtained

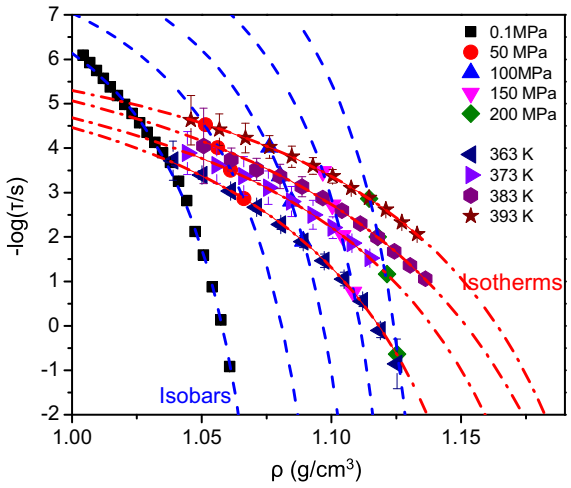

Fig. 7. Dependence of "isothemal" (red dash-dotted lines) and "isobaric" (blue dashed lines) segmental relaxation times on density.

from PVT measurements. The $T_g(P)$ dependence can be described according to the empirical equation,

$$T_g(P) = T_g(0)\left(1+\frac{\kappa}{\lambda}P\right)^{1/k} \quad (12)$$

first proposed by Simon and Glatzel [36] for the melting of solidified gases under pressure and subsequently employed by Andersson and Andersson [37] and others [25,26,38] to describe the $T_g(P)$ of glass-forming systems. In the above equation, $T_g(0)$ is the temperature (at $P = 0.1$ MPa) where the characteristic relaxation time of each process corresponds to 100 s, and κ and λ are polymer specific parameters (the parameters are summarized in Table 1, where the values of the initial slopes $(dT/dP)_{P \to 0}$ are also given).

In addition, Casalini *et al.* [39] obtained the same ratio from purely thermodynamic data of the equation of state as the ratio of the isobaric, $\alpha_P = (\partial \ln V/\partial T)_P$, to the isochronic, $\alpha_\tau = (\partial \ln V/\partial T)_\tau$, thermal expansion coefficients as

$$\mathfrak{R} = \Delta E^{\#}/\Delta H^{\#} = [1-\alpha_P/\alpha_\tau]^{-1} \quad (13)$$

Poly(*n*-alkyl methacrylates), with the systematic variation of the alkyl side group, are a unique system for investigating possible

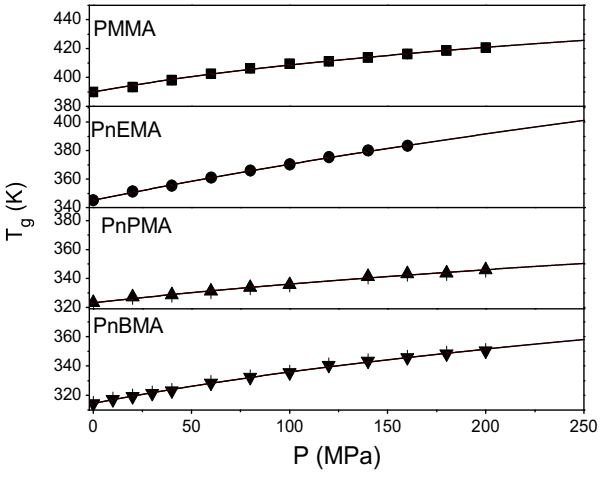

Fig. 8. Pressure dependence of the glass temperature of lower poly(*n*-alkyl methacrylates) as obtained from PVT measurements.

Table 1
Parameters of the pressure dependence of the glass temperature for the lower poly(*n*-alkyl methacrylates).

Polymer	M_W (g/mol)	$T_g(0)$ K	κ	λ (MPa)	dT_g/dP (K/GPa)
PMMA	40,000	389.0 ± 2.0	12.31 ± 1.81	1590 ± 90	246
PEMA	2000	345.2 ± 2.0	3.75 ± 0.45	1240 ± 25	279
PPMA	48,000	323.2 ± 1.5	8.53 ± 1.96	2160 ± 120	150
PBMA		296.0 ± 4.0	6.81 ± 0.75	1200 ± 50	263

correlations between various dynamic quantities. Herein we investigate a possible correlation between the value of $\mathfrak{R}$ at T_g and the pressure coefficient of T_g. This is shown in Fig. 9 for the majority of polymers investigated so far where the characteristic ratio is obtained by *PVT* measurements (Eq. (13)) and by DS (Eq. (11)). The figure displays a broad correlation between the characteristic ratio and the pressure-sensitivity of the glass temperature. It basically shows that systems with a low value of the characteristic ratio, *i.e.*, systems where the segmental dynamics are controlled predominantly by volume and to a lesser extent by temperature, as for example in BPA-PC [25], display also a strong pressure dependence of their glass temperature. This is understandable as in such systems the dynamics are governed predominantly by inter-molecular correlations and these are most susceptible to pressure changes. On the other hand, systems such as PE (obtained from simulations) or the present PPMA, have higher values of the characteristic ratio suggesting that intra-molecular correlations prevail. In such systems the pressure coefficient of the glass temperature is the smallest.

A recent investigation on the origin of the heterogeneous dynamics of PBMA by single molecule spectroscopy and dielectric spectroscopy [40] revealed spatial and temporal heterogeneous dynamics with the contribution from the former to dominate in the range from T_g to T_g + 20 K. In view of the predominant intramolecular segmental dynamics in PPMA it would be of interest to explore the origin of the heterogeneous dynamics in this polymer as well.

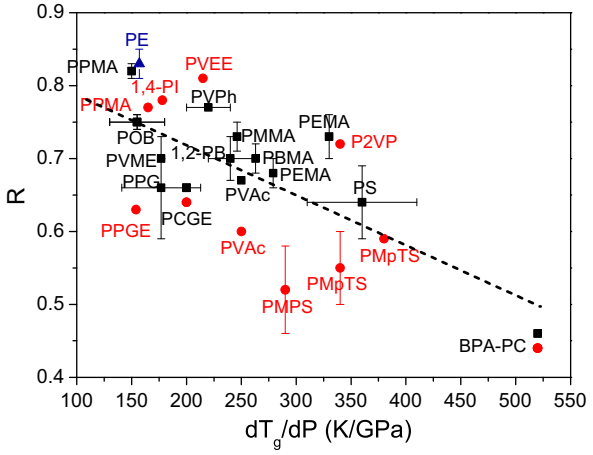

Fig. 9. Dependence of the ratio of the constant-volume activation energy ($Q_V(T,P)$) to the constant-pressure activation energy ($Q_P(T,P)$) to the pressure coefficient of T_g for several polymers. (Black symbols): *R* is obtained from *PVT* measurements; (red symbols): *R* is obtained from DS; (blue symbol, PE): *R* is obtained from simulations. The dashed line is the result of a fit to the PVT data. (PMMA) poly(methylmethacrylate), (PEMA) poly(ethylmethacrylate), (PPMA) poly(propylmethacrylate), (PBMA) poly(butylmethacrylate), (PMpTS) poly(methyl-*p*-totyl siloxane), (PMPS) poly(methyl phenyl siloxane), (PVAc) polyvinylacetate, (BPA-PC) bisphenol-A-polycarbonate, (P2VP) poly(2-vinylpyridine), (PVEE) poly(vinylethylether), (POB) poly(oxybutylene), (PVPh) poly(4-vinyl phenol), (PVME) poly(vinyl methyl ether), (PPG) poly(propylene glycol), (PPGE) poly(phenol glycidyl ether)-*co*-formaldehyde, (PCGE) poly(*o*-cresol glycidyl ether)-co-formaldehyde, (PE) polyethylene, (PS) polystyrene, (1,4-PI) 1,4-polyisoprene, and (1,2-PB) 1,2-polybutadiene.

5. Conclusion

By employing lower poly(*n*-alkyl mathecrylates) and in particular, PPMA, we have examined the origin of the segmental dynamics by applying both *T* and *P* as thermodynamic variables. We find that for PPMA the segmental dynamics is controlled mainly by temperature via the intramolecular barriers ($\mathfrak{R} \sim 0.82$). At the same time the pressure coefficient of the glass temperature is one of the lowest ever reported ($dT_g/dP = 150$ K/GPa). Based on this finding we examined a possible correlation between the value of $\mathfrak{R}$ at T_g and the pressure coefficient of T_g, dT_g/dP, for a broad range of polymers investigated both by PVT and DS. We find a broad correlation that has as extremes, BPA-PC from one side, and PE and the lower poly(*n*-alkyl methacrylates) from the other side. This suggests that changes in the intra- vs inter-molecular polymer dynamics may be reflected in the pressure sensitivity of the glass temperature.

Acknowledgments

This work was co-financed by the E.U.—European Social Fund and the Greek Ministry of Development—GSRT in the framework of the program THALIS (MIS 379436). The current work was supported by the Research unit on Dynamics and Thermodynamics of the UoI co-financed by the European Union and the Greek state under NSRF 2007-2013 (Region of Epirus, call 18).

References

[1] N.G. McCrum, B.E. Read, G. Williams, Anelastic and Dielectric Effects in Polymeric Solids, Wiley, New York, 1967.
[2] Y. Ishida, K. Yamafuji, Kolloid Z. 177 (1961) 97.
[3] (a) G. Williams, Trans. Faraday Soc. 60 (1964) 1548.
(b) G. Williams, ibid, 60 (1964) 1556.
[4] H. Sasabe, S. Saito, J. Polym. Sci. A-2 6 (1968) 1401.
[5] Y. Ishida, J. Polym. Sci. A-2 7 (1969) 1835.
[6] S.C. Kuebler, D.J. Schaefer, C. Boeffel, U. Pawelzik, H.W. Spiess, Macromolecules 30 (1997) 6597.
[7] G. Floudas, P. Stepanek, Macromolecules 31 (1998) 6951.
[8] K. Mpoukouvalas, G. Floudas, G. Williams, Macromolecules 42 (2009) 4690.
[9] M. Beiner, H. Huth, Nat. Mater. 2 (2003) 595.
[10] D. Gomez, A. Alegria, A. Arbe, J. Colmenero, Macromolecules 34 (2001) 503.
[11] M. Wind, R. Graf, A. Heuer, H.W. Spiess, Phys. Rev. Lett. 91 (2003) 155702/1–155702/4.
[12] K.L. Ngai, T.R. Gopalkrishnan, M. Beiner, Polymer 47 (2006) 7222.
[13] M. Mierzwa, G. Floudas, P. Stepanek, G. Wegner, Phys. Rev. B 62 (2000) 14012.
[14] M. Mierzwa, G. Floudas, IEEE Trans. Dielectr. Electr. Insul. 8 (2001) 359.
[15] F. Kremer, A. Schönhals (Eds.), Broadband Dielectric Spectroscopy, Springer, Berlin, 2002.
[16] G. Floudas, Prog. Polym. Sci. 29 (2004) 1143.
[17] G. Floudas, in: K. Matyjaszewski, M. Möller (Eds.), Dielectric spectroscopy, Polymer Science: A Comprehensive Reference, vol. 2.32, Elsevier BV, Amsterdam, 2012, pp. 825–845.
[18] S. Havriliak, S. Negami, J. Polym. Sci. C 14 (1966) 99.
[19] G. Williams, D.C. Watts, in: P. Diehl, E. Flick, E. Kosfeld (Eds.), NMR Basic Principles and Progress, vol. 4, Springer, Berlin, 1971, p. 271.
[20] P. Zoller, D. Walsh, Standard Pressure–Volume–Temperature Data for Polymers, Technomic Publishing Co. Inc., 1995. 43.
[21] R.L. Miller, R.F. Boyer, J. Heijboer, J. Polym. Sci. Polym. Phys. Ed. 22 (1984) 2021.
[22] G. Floudas, M. Paluch, A. Grzybowski, K.L. Ngai, Molecular Dynamics of Glass-Forming Systems. Effects of Pressure, Springer, 2011.
[23] M. Paluch, A. Patkowski, E.W. Fischer, Phys. Rev. Lett. 85 (2000) 2140.
[24] G. Floudas, K. Mpoukouvalas, P. Papadopoulos, J. Chem. Phys. 124 (2006) 074905.
[25] K. Mpoukouvalas, N. Gomopoulos, G. Floudas, C. Herrmann, A. Hanewald, A. Best, Polymer 47 (2006) 7170.
[26] P. Papadopoulos, D. Peristeraki, G. Floudas, G. Koutalas, N. Hadjichristidis, Macromolecules 37 (2004) 8116.
[27] G. Floudas, T. Reisinger, J. Chem. Phys. 111 (1999) 5201.
[28] G. Floudas, C. Gravalides, T. Reisinger, G. Wegner, J. Chem. Phys. 111 (1999) 9847.
[29] M. Naoki, H. Endou, K. Matsumoto, J. Phys. Chem. 91 (1987) 4169.
[30] R. Casalini, C.M. Roland, Phys. Rev. E. 69 (2004) 062501.
[31] C.M. Roland, M. Paluch, T. Pakula, R. Casalini, Philos. Mag. 84 (2004) 1573.
[32] R. Casalini, C.M. Roland, Macromolecules 46 (2013) 6364.
[33] C.M. Roland, S. Hensel-Bielowka, M. Paluch, R. Casalini, Rep. Prog. Phys. 68 (2005) 1405.
[34] J. Dudowicz, K. Freed, J.F. Douglas, J. Chem. Phys. 123 (2005) 111102.
[35] K.L. Ngai, C.M. Roland, Macromolecules 26 (1993) 6824.
[36] F.E. Simon, G.Z. Glatzel, Anorg. Allg. Chem. 178 (1929) 309.
[37] S.P. Andersson, O. Andersson, Macromolecules 31 (1998) 2999.
[38] K. Mpoukouvalas, G. Floudas, Phys. Rev. E. 68 (2003) 031801.
[39] R. Casalini, C.M. Roland, J. Chem. Phys. 119 (2003) 4052.
[40] A. Deres, G. Floudas, K. Müllen, M. Van der Auweraer, F. De Schryver, J. Enderlein, H. Uji-i, J. Hofkens, Macromolecules 44 (2011) 9703.